Inorganic Chemistry

pubs.acs.org/IC Article

Trimethylsilyldiazomethane Disassembly at a Three-Fold Symmetric Iron Site

Austin D. Chivington, Sammie Squire, Nobuyuki Yamamoto, Maren Pink, Morgan D. Griffith, Jess Fletcher, Yafei Gao, Joseph M. Zadrozny, and Jeremy M. Smith*

Cite This: https://doi.org/10.1021/acs.inorgchem.4c00604 Read Online

ACCESS | Metrics & More | Article Recommendations | Supporting Information

ABSTRACT: The reaction of equimolar trimethylsilyldiazomethyllithium (LiTMSD) with high spin (S = 2) $PhB(AdIm)_3FeCl$ ($PhB(AdIm)_3^-$ = tris(3-adamantylimidazol-2-ylidene)phenylborate) affords the corresponding N-nitrilimido complex $PhB(AdIm)_3Fe{-}N{=}N{=}C(SiMe_3)$. This complex can be converted to the thermodynamically more favorable C-isocyanoamido isomer $PhB(AdIm)_3Fe{-}C{=}N{=}N(SiMe_3)$ by reaction with an additional equivalent of LiTMSD. While the iron(II) complexes are four-coordinate, the diazomethane is bound side-on in the iron(I) congener $PhB(AdIm)_3Fe(N,N'\text{-}\kappa^2\text{-}N_2C(H)Si(CH_3)_3)$. The latter complex adopts high spin (S = 3/2) ground state and features an unusually weak C−H bond. Photolysis of the iron(II) complexes induces N═N bond cleavage, with the iron(II) cyanide $PhB(AdIm)_3Fe{-}C{\equiv}N$ and iron(IV) nitride $PhB(AdIm)_3Fe{\equiv}N$ complexes being the major products of the reaction. The same products are obtained when the iron(I) complex is photolyzed or treated with a fluoride source. The trimethylsilyldiazomethane-derived ligand disassembly reactions are contrasted with those observed for related tris(carbene)-amine complexes.

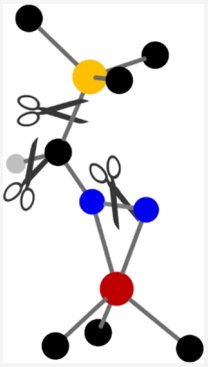

INTRODUCTION

Diazoalkane (N_2CR_2) complexes are conceptually appealing as an entry point to the synthesis of metal−carbon multiple bonds, where the expulsion of N_2 gas provides a strong thermodynamic driving force. For example, nickel carbene complexes are accessible through both photochemical and Lewis acid-catalyzed loss of N_2 from the corresponding diazomethane complexes.[1] However, this same diazo group may also be associated with undesired complications, including two commonly observed coordination modes: "end-on" in which the metal is σ-bonded through the terminal nitrogen atom of the diazoalkane, and "side-on" via the diazoalkane π-system. More exotically, the metal can function as a substituent on the diazoalkane in the form of a C-bound diazoalkane complex.[2,3]

We (and others) have shown the utility of rigid, strongly donating tris(carbene)borate ligands for the isolation of late transition metal complexes bearing metal−ligand multiple bonds.[2−5] By stabilizing a 3-fold symmetric environment at a four-coordinate metal center, these ligands create a d-orbital manifold that diminishes destabilizing σ^* and π^* interactions with the multiply bonded ligand. Consequently, we have been able to isolate tris(carbene)borate iron complexes featuring terminal oxo,[5] imido,[6] sulfido,[7] and nitrido[8] ligands.

In light of this precedent, we were interested in extending the library of tris(carbene)borate iron complexes to include iron−carbon multiple bonds. Indeed, the synthetic flexibility inherent to trimethylsilyldiazomethane provides a tantalizing motivation to use this molecule as a synthon for accessing iron−carbon multiple bonds. Specifically, in addition to N_2 extrusion, access to iron−carbon multiple bonds via the deprotonation and desilylation of trimethylsilyldiazomethane-derived ligands can also be envisioned. Perhaps surprisingly, isolable iron complexes bearing a trimethylsilyldiazomethane-derived ligand are rare. While trimethylsilyldiazomethane has been used to install a bridging alkylidene ligand in a diiron complex,[9] similar reactivity has yet to be observed in mononuclear iron complexes.[10,11] For example, (^{iPr}PDI)Fe−N═N−C(H)$SiMe_3$ (^{iPr}PDI = 2,6-(2,6-^{i}Pr$_2$C$_6$H$_3$N═CMe)$_2$C$_5$H$_3$N) reacts intramolecularly to eliminate Me_4Si,[10] while $[(TIMEN^{mes})Fe(-N{=}N{=}CSiMe_3)]^+$ ($TIMEN^{mes}$ = tris[2-(3-mesityl-imidazole-2-ylidene)ethyl]amine) reacts with fluoride to generate the corresponding iron(IV) nitride complex along with CN^- and Me_3SiF.[11] The paucity of iron complexes bearing trimethylsilyldiazomethane-derived ligands, along with their divergent reactivity, provides additional impetus for our studies.

In this work, we report our investigations into iron tris(carbene)borate complexes with trimethylsilyldiazomethane-derived ligands. In contrast to previous reports, a number of binding modes are observed on the same metal scaffold, with the oxidation state of the metal dictating the denticity of the ligand. While we have been unable to coax the

Received: February 9, 2024
Revised: May 7, 2024
Accepted: May 13, 2024

Scheme 1

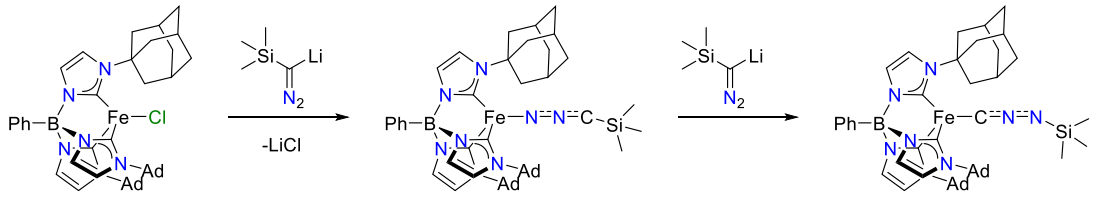

formation of iron−carbon multiple bonds by thermal or photochemical means, we observe interesting differences with related complexes, highlighting the nuanced reactivity of trimethylsilyldiazomethane and its ligands.

RESULTS AND DISCUSSION

Synthesis of iron(II) Nitrilimido and Isocyanoamido Complexes. In solution, trimethylsilyldiazomethyllithium (LiTMSD) exists as an equilibrium mixture of *N*- and *C*-lithiated isomers, with the equilibrium position dependent upon the coordinating ability of the solvent.[9,12] The *C*-lithiated ion is favored for coordinating solvents that are better able to solvate the lithium cation. Despite these considerations, we observe that the reaction of equimolar LiTMSD with $PhB(AdIm)_3FeCl$ (**1**) in THF provides the high spin (S = 2) *N*-nitrilimido complex $PhB(AdIm)_3Fe{-}N{=}N{=}C(SiMe_3)$ (**2**) as the sole iron-containing product (Scheme 1). This complex can also be synthesized by the addition of trimethylsilyldiazomethane to $PhB(AdIm)_3FeNH_2$ (which is readily prepared by addition of sodamide to $PhB(AdIm)_3FeCl$, see Supporting Information for more details).

The molecular structure of **2**, as determined by single crystal X-ray diffraction, reveals a pseudotetrahedral iron center with a terminal *N*-nitrilimido ligand (Figure 1).[13] The nitrilimido structural metrics (N=N 1.123(2) Å; N=C 1.203(3) Å) are consistent with an allenic electronic structure. This linear allenic core of the ligand is also consistent with this assignment (N−N−C 173.4(2)°), although the ligand substituents are bent away from linearity (Fe−N−N 150.7(1)° and N−C−Si 143.5(2)°). It is interesting to compare this structure with that of the related iron *N*-nitrilimido complex $[(TIMEN^{mes})Fe(N{=}N{=}CSiMe_3)]^+$.[11] While the nitrilimido bond distances of both complexes are similar, in $[(TIMEN^{mes})Fe(N{=}N{=}CSiMe_3)]^+$, the ligand is nearly linear (Fe−N−N 177.0(2); N−N−C 179.7(4); N−C−Si 179.3(4)°).[33] Here, it is worth noting that computational studies have shown that the thermal barrier between the two major resonance forms of the *N*-nitrilimido ligand, namely, propargylic and allenic, is relatively small (~2.5 kJ mol^{-1}).[14] Thus, we suggest a dominant allenic resonance for **2** and that the bending results from packing forces in the solid state.[35] The other structural metrics for the complex are unremarkable, with the Fe−N (2.005(1) Å) and Fe−C bond distances (2.070(1) − 2.117(1) Å) being typical for a high spin (S = 2) iron(II) tris(carbene)borate complex.

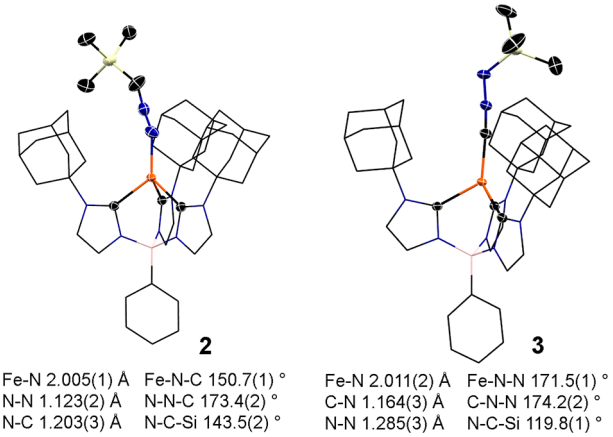

Figure 1. X-ray crystal structures of **2** and **3**, along with the selected bond distances and bond angles. Thermal ellipsoids are at 50% probability; hydrogen atoms omitted and most of the tris(carbene)-borate ligand shown as wireframe for clarity. Black, orange, blue, and yellow ellipsoids represent carbon, iron, nitrogen, and silicon atoms, respectively.

Solution characterization of **2** is consistent with the solid-state structure. The ^1H NMR spectrum of the complex is consistent with a 3-fold symmetric structure, with a diagnostic resonance at δ = 34 ppm assigned to the protons of the trimethylsilyl group. The high spin state is characterized by Evans' method (μ_{eff} = 5.0(2) μ_B). Vibrational spectroscopy confirms the presence of the *N*-nitrilimido ligand ($\nu_{N=N}$ = 2047 cm^{-1}). Complex **2** has high thermal stability, with no spectral changes occurring on heating for 3 h at 50 °C.

Unexpectedly, complex **2** reacts with additional LiTMSD to afford the *C*-isocyanoamido isomer $PhB(AdIm)_3Fe{-}C{=}N{=}N(SiMe_3)$ (**3**), as determined by single crystal X-ray diffraction (Scheme 1, Figure 1).[8] Compared to the *N*-nitrilimido ligand in **2**, the *C*-isocyanoamido ligand in **3** has a shorter C=N bond (1.164(3) Å) and a longer N=N bond (1.285(3) Å). While the C=N=N core in **3** is also linear (174.2(2)°), the N−N−Si bond angle (119.8(1)°) is significantly smaller than the related N−C−Si angle in **2** (143.5(2)°), indicative of lone-pair character at the silicon-bound nitrogen atom. The C=N bond distance in **3** is the same as that observed for the only other structurally characterized *C*-isocyanoamido complex (TIMEN*)CoC=N=NMes.[38] However, the N=N distance in the latter complex (1.332(2) Å) is longer than that in **3**. As with **2**, the Fe−C distances to the tripodal ligand (2.071(1)−2.094(1) Å) and isocyanoamido (2.011(2) Å) ligands are in the range observed for a high spin (S = 2) iron(II) tris(carbene)borate complex.

Complex **3** is also spectroscopically distinct from the *N*-nitrilimido complex **2**. Most notably, the diagnostic resonance of the trimethylsilyl protons in the ^1H NMR spectrum is shifted upfield from 34 ppm in **2** to 18 ppm in **3**. Additionally, vibration spectroscopy is consistent with the shorter N−N bond, as the IR spectrum shows that the band attributed to the isocyanoamido ligand is red-shifted ($\nu_{N=N}$ = 2062 cm^{-1}) from the related band in **2**.

The mechanism by which **3** is formed is not clear, although DFT calculations (B3LYP/def2-TZVP) reveal that this isomer is thermodynamically favored by 6.7 kcal/mol (Table S3). The formation of **3** is only facilitated by stoichiometric LiTMSD

https://doi.org/10.1021/acs.inorgchem.4c00604
Inorg. Chem. XXXX, XXX, XXX−XXX

and is not induced by other bases such as $KN(SiMe_3)_2$ or $NaNH_2$. Monitoring the reaction by ^1H NMR spectroscopy reveals that the additional LiTMSD is completely consumed; however, attempts to determine the byproducts of the reaction have been unsuccessful. These observations suggest that the reaction mechanism involves coordination of the second trimethylsilyldiazomethyl ligand to iron. Akin to observations for trimethylsilyldiazomethyl ligand isomerization in a diiron complex,[9] we speculate that the carbon atom of the bound trimethylsilyldiazomethyl ligand binds to the lithium ion, facilitating delivery of the *C*-bound isomer to iron. However, since the reaction is not catalytic in LiTMSD, a simple ligand exchange mechanism is unlikely. Unfortunately, we have been unable to determine the fate of the additional trimethylsilyldiazomethyl ligand, hindering additional mechanistic insight. Previously, isocyanoamido ligand formation in (TIMEN*)-CoC=N=NMes was induced by the reaction of the nitrilimido complex $[(TIMEN^{mes})Co(N{=}N{=}CSiMe_3)]^+$ with fluoride.[15] However, reaction of **2** with fluoride sources does not provide tractable products.

Synthesis, Characterization, and Reactivity of an Iron(I) Azomethane Complex. The previously reported iron(I) dinitrogen complex $PhB(AdIm)_3FeN_2$ (**4**) reacts with trimethylsilyldiazomethane in THF to afford $PhB(AdIm)_3Fe(N,N'\text{-}\kappa^2\text{-}N_2C(H)Si(CH_3)_3)$ (**5**); see Scheme 2. The structure

Scheme 2

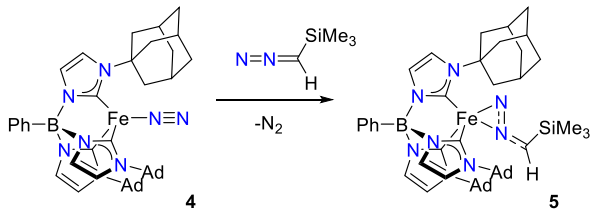

of **5** was elucidated by single crystal X-ray diffraction, revealing a five-coordinate complex with a side-bound trimethylsilyldiazomethane ligand (Figure 2). The diazoalkane N=N (1.238(6) Å) and C=N (1.314(9) Å) bond distances suggest that the dominant resonance form is maintained upon binding.

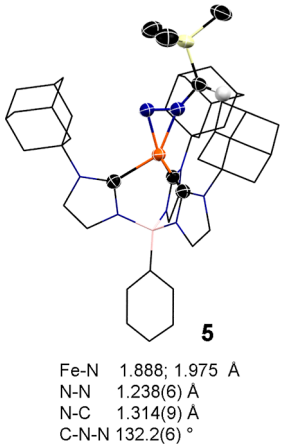

Figure 2. X-ray crystal structure of **5**. Thermal ellipsoids are at 50% probability; most of the hydrogen atoms omitted and most of the tris(carbene)borate ligand shown as wireframe for clarity. Black, orange, blue, and yellow ellipsoids represent carbon, iron, nitrogen, and silicon atoms, respectively.

Indeed, the N=N bond distance is shorter than for other reported side-bound trimethylsilyldiazomethane complexes, namely, $Cp_2{*}Ti(N_2C(H)SiMe_3)$ (1.276(3) Å)[16] and $(BDI)\text{-}Cr(CH_2SiMe_3)(N_2C(H)SiMe_3)$ (1.332(3) Å),[17] suggesting a lower degree of π-backbonding in **5**. The N=N bond distance is also shorter than in the iron diphenylazomethane complex $(^{iPr}PDI)Fe(N_2CPh_2)$ (1.280(3) Å).[18] It is remarkable that side-on binding is favored over an end-on mode, despite the large steric encumbrance of the very bulky tris(carbene)borate ligand. It is worth noting that five-coordinate complexes with this tris(carbene)borate ligand are known, namely, the iron(I) dicarbonyl complex $PhB(AdIm)_3Fe(CO)_2$[19] and the iron(III) disulfide $PhB(AdIm)_3Fe(\kappa^2\text{-}S_2)$.[5]

Interestingly, the Fe−C distances in **5** (2.102−2.084 Å) are longer than in the related iron(I) complex $PhB(MesIm)_3Fe(CO)_2$ (1.978(5) − 2.007(5) Å), which is low spin (S = 1/2), implicating a different electronic structure for **5**. Variable temperature dc magnetic susceptibility data were collected at three different fields (0.1, 0.5, and 1.0 T) to probe the ground-state spin of complex **5**. At 300 K, the value of $\chi_M T$ is 2.45 cm^3 K/mol at 0.1 T, which is close to the expected value of 2.46 for an S = 3/2 system with g = 2.29 (Figure 3). With decreasing temperature, $\chi_M T$ stays relatively constant until 50 K, wherein $\chi_M T$ begins to drop and ultimately reaches 1.79 cm^3 K/mol at 2 K, likely as a result of zero-field splitting. Fitting these data with PHI[20] provided spin-Hamiltonian values g_{iso} = 2.30 and D = −12.9 cm^{-1}.

Reduced magnetization data provided nonsuperimposable isofield lines, also suggesting the presence of zero-field splitting (Figure 4). The spin-Hamiltonian values suggested also a large zero-field splitting, though the fitted parameters from PHI were different than the 2−300 K dc $\chi_M T$ data set: g_{iso} = 2.62, D = −42.91 cm^{-1} and $|E|$ = 0.03 cm^{-1}. The discrepancy between the $\chi_M T$ and magnetization data fitting results suggests that the sign and magnitude of D are not precisely defined. However, we can confidently infer that **5** is anisotropic and the magnitude of D is between 10 and 40 cm^{-1}, in line with literature expectations for this ion. For example, low-spin five-coordinate iron(I) complexes are reported with g_{iso} = 2.03−2.06 determined by EPR spectroscopy,[21] and high-spin, four-coordinate iron(I) complexes can show g values of 2.13 up to 3.81 by electron paramagnetic resonance (EPR) spectroscopy.[22,23] Parameterization of D in one of these complexes revealed a D up to 20 cm^{-1}.[20] A separate high-spin iron(I) tris(thiolate) complex also produced very large g values (up to 3.41), indicative of zero-field splitting effects in its S = 3/2 ground state.[24] Factors including coordination number, symmetry, and ligand field strength limit direct comparison of **5** to other iron(I) complexes, but the foregoing literature evidence clearly supports our conclusion that **5** is anisotropic.

The zero-field ^{57}Fe Mössbauer spectrum at 273 K reveals an asymmetric doublet at δ = 0.75 mm/s (ΔE_Q = 2.50 mm/s). The positive isomer shift is consistent with high spin Fe(I), with the asymmetry indicative of a noninteger spin complex. The isomer shift is distinct from that for the S = 3/2 iron(III) disulfide complex $PhB(AdIm)_3Fe(\kappa^2\text{-}S_2)$ (δ = 0.42, ΔE_Q = 2.54 mm/s), further supporting the low-valent oxidation state assignment.[5] DFT calculations (B3LYP/def2-TZVP) reproduce the observed S = 3/2 ground spin state, with the S = 1/2 state higher in energy by 8.7 kcal/mol (Table S3). In addition, the DFT-computed ^{57}Fe Mössbauer spectral parameters for the S = 3/2 state (δ = 0.61 mm/s, ΔE_Q = −2.08 mm/s) are in reasonable agreement with those observed experimentally.

https://doi.org/10.1021/acs.inorgchem.4c00604
Inorg. Chem. XXXX, XXX, XXX−XXX

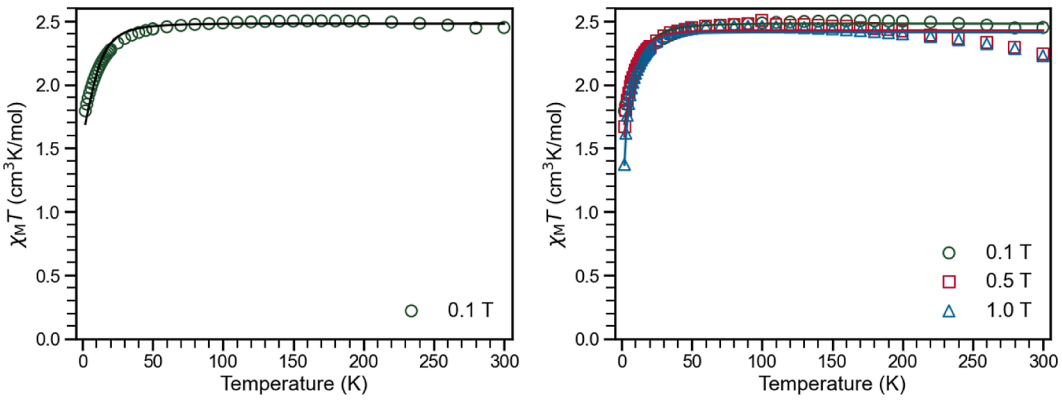

Figure 3. (Left) Variable-temperature dc susceptibility ($\chi_M T$) data for **5** collected under an applied magnetic field of 0.1 T. The solid black line is a fit generated using PHI to extract spin Hamiltonian parameters $g_{iso} = 2.30$, $D = -12.88$ cm^{-1}. (Right) Variable-field, variable-temperature $\chi_M T$ data collected at 0.1, 0.5, and 1 T magnetic fields. Solid lines are best simulations of the data with $g_{iso} = 2.27$ and $|D| = 9.95$ cm^{-1} for 0.5 T and $g_{iso} = 2.27$ and $|D| = 10.13$ cm^{-1} for 1 T.

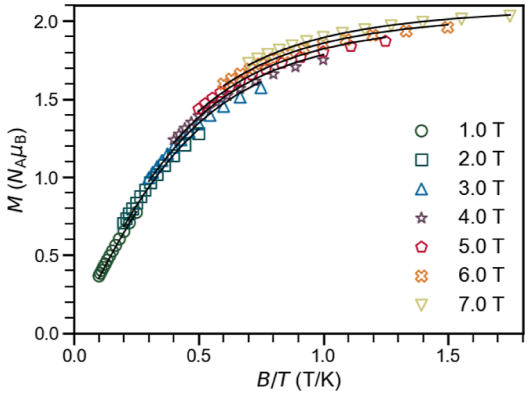

Figure 4. Reduced magnetization (M) data for **5** under applied magnetic fields (B) of 1−7 T and temperature range of 4−10 K. Solid black lines are fits generated using PHI to extract spin Hamiltonian parameters $g_{iso} = 2.62$, $D = -43$, and $|E| = 0.03$ cm^{-1}.

The ^{1}H NMR spectrum of **5** reveals seven paramagnetically shifted resonances, indicating a three-fold symmetric structure and suggesting that the five-coordinate complex is fluxional in solution. A broad resonance at $\delta = 9$ ppm can be uniquely assigned to the protons of the trimethylsilyl group. The trimethylsilyldiazomethane ligand is also observed by vibrational spectroscopy ($\nu_{N=N} = 2059$ cm^{-1}), where the stretching frequency occurs at lower frequency than that of free diazomethane ($\nu_{N=N} = 2070$ cm^{-1}). Complex **5** has remarkable thermal stability, being persistent in benzene-d_6 at 80 °C for at least 3 days, and with no evidence for decomposition after months in the solid state at room temperature. There is no evidence for N_2 extrusion under these conditions.

It is notable that complexes **5** and **2**/**3** differ by a single hydrogen atom, suggesting that they could be interconverted by formal hydrogen atom transfer reactions. This hypothesis is supported by DFT calculations, which provide an estimate for the gas phase C−H BDFE (B3LYP/def2-TZVP)

$$\mathrm{PhB(AdIm)_3Fe}(N, N' - \kappa^2 2 - \mathrm{N2C(H)Si(CH3)3} \rightarrow \mathrm{PhB(AdIm)_3Fe - N = N = C(SiMe_3)} + \mathrm{H\bullet}$$

$$\Delta G = 55 \text{ kcal/mol}$$

This prediction is borne out experimentally, where we observe that complex **5** reacts with both Gomberg's dimer (a source of the triphenylmethyl radical) and TEMPO to provide **2**, along with the triphenylmethane (C−H BDFE = 75.7 kcal/mol) and TEMPO-H (O−H BDFE = 65.5 kcal/mol), respectively.[25] The unusual weakness of the C−H bond in **5** is notable,[25] being significantly less than the weak C−H bond in 1,3-cyclohexadiene (BDFE = 67.8 kcal/mol).[26] This value is comparable with those observed for some weak metal-hydride bonds, e.g., $CpCr(CO)_3H$ (BDFE = 54.9 kcal/mol)[27] and $(dppm)V(CO)_4H$ (BDFE = 51.1 kcal/mol).[28]

Photochemical Transformations. As noted above, complexes **2**, **3**, and **5** have high thermal stability and attempts to thermally promote N_2 loss have been unsuccessful. Inspired by observations for low-coordinate nickel complexes,[1] we investigated irradiation as a strategy to facilitate N_2 extrusion in the creation of iron−carbon multiple bonds.

Photolysis of iron(II) *N*-nitrilimido complex **2** with an 800 W XeHg broadband lamp converts the initial golden yellow solution to a brilliant salmon color. Analysis of the reaction products by ^{1}H NMR spectroscopy reveals the formation of the iron(II) cyanide complex **6** and iron(IV) nitrido **7** in

Scheme 3

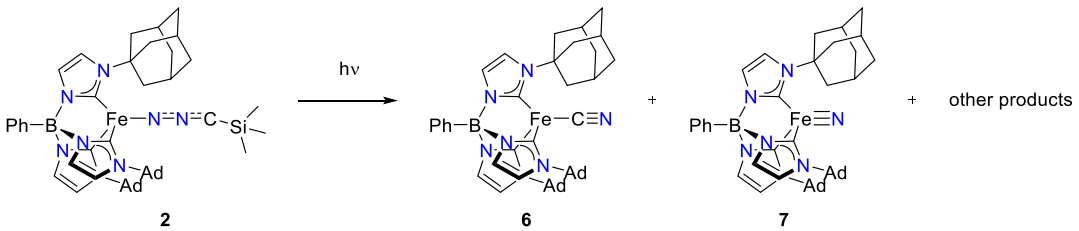

https://doi.org/10.1021/acs.inorgchem.4c00604
Inorg. Chem. XXXX, XXX, XXX−XXX

approximately 1:1 ratio (Scheme 3). While these complexes could not be physically separated, they could be independently synthesized, allowing for their complete characterization, including by single-crystal X-ray diffraction. We have been unable to determine the other product(s) of the reaction.

Complex **6** can be prepared by a similar strategy as our previously reported synthetic route for PhB(^{t}BuIm)$_3$FeCN. Thus, reaction of equimolar anhydrous Me_4NF with PhB(AdIm)$_3$FeCl affords the corresponding iron(II) fluoride complex PhB(AdIm)$_3$FeF, which has been structurally and spectroscopically characterized. The fluoride complex reacts in turn with stoichiometric trimethylsilyl cyanide to form the high spin (S = 2) complex PhB(AdIm)$_3$Fe−C≡N (**6**). This complex shows similar structural and spectroscopic characteristics to PhB(^{t}BuIm)$_3$Fe−C≡N (Figure 5),[29] with the cyanide ligand observed by IR spectroscopy (ν_{CN} = 2051 cm^{-1}).

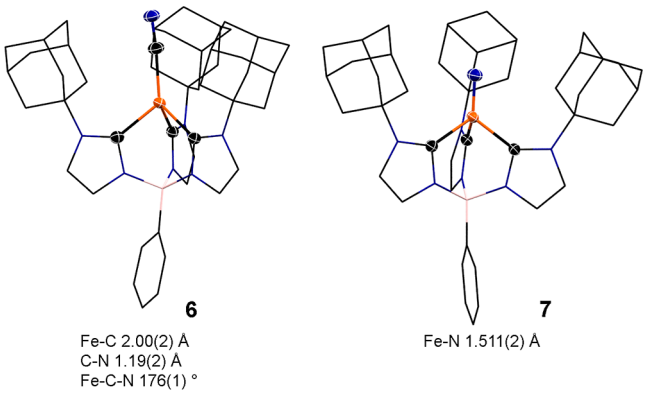

Figure 5. X-ray crystal structures of **6** and **7**. Thermal ellipsoids are at 50% probability; most of the hydrogen atoms omitted and most of the tris(carbene)borate ligand shown as wireframe for clarity. Black orange, and blue ellipsoids represent carbon, iron, and nitrogen atoms, respectively.

Complex **7** is also prepared following our previously reported synthetic route. Here, treatment of PhB(AdIm)$_3$FeCl with an excess of sodium azide affords the iron(II) complex PhB(AdIm)$_3$FeN$_3$ (ν_{NNN} = 2068 cm^{-1}), which is photochemically converted to the diamagnetic iron(IV) nitride. The molecular structure of **6** shows similar metrics to those of previously reported iron(IV) tris(carbene)borate nitrides, along with spectroscopic properties that are also in line with this class of complex.[8]

It is interesting to compare the reactivity of **2** with that of the related N-nitrilimido complex [(TIMEN^{mes})Fe(N$_2$CSiMe$_3$)]$^+$.[9] For the latter complex, the nitrilimido ligand is desilylated by NBu_4F to afford the corresponding iron(IV) nitride, with concomitant formation of Me_3SiF and NBu_4CN. The nitride complex is not formed through irradiation. By contrast, while irradiation of **2** provides the iron(IV) nitride product, reaction with anhydrous NBu_4F gives an intractable mixture of paramagnetic products. While the precise factor(s) leading to these differences are not clear, it does highlight the dramatic impact of the supporting tris(carbene) ligand on the reactivity of the N-nitrilimine ligand.

Similar irradiation of the iron(II) isocyanoamido complex **3** also provides iron(II) cyanide **6**, along with unidentified paramagnetic complex(es). In this case, the iron(IV) nitride complex **7** is not observed. The same products are formed when **3** is heated, although the rate of reaction is slower than under photochemical conditions. Complexes **6** and **7** are also formed when the iron(I) azomethane complex **5** is irradiated. In contrast to the iron(II) complexes, this complex reacts cleanly with Me_4NF, again yielding complexes **6** and **7**.

CONCLUSIONS

In this work, we demonstrated multiple coordination modes for trimethylsilyldiazomethane-derived ligands at an iron tris(carbene)borate fragment. Notably, the denticity of the ligand is dictated by the oxidation state of the metal ion. Monodentate binding modes are observed for the iron(II) complexes **2** and **3**, whereas a side-bound κ^2-N,N' bidentate mode is observed for complex **5**. The latter binding mode can be attributed to the superior π-backbonding abilities of the low-valent metal ion, which favors interaction of the N=N π^* orbital. It is also interesting that the N-bound trimethylsilylazomethyl ligand in **2** is converted to the thermodynamically favored C-bound form in **3** through the addition of a second equivalent of LiTMSD.

As stated in the introduction, trimethylsilyldiazomethane is an intriguing reagent for creating metal−carbon multiple bonds because a number of strategies can be envisioned, including stepwise C−H and C−F bond cleavage, or through direct N_2 extrusion. In contrast to tris(carbene)amine complexes, thermal routes toward disassembly of the diazomethane ligand in tris(carbene)borate complex **2** are unproductive as by photolysis in N=N bond cleavage is only observed. Similar results are obtained for **3** and the iron(I) complex **5**, although both thermal and photochemical conditions are productive. Subtle steric and electronic differences between the two tris(carbene) ligands appear to have dramatic consequences on the reactivity of azomethane ligand. While we have been able to leverage the deprotonation and desilylation chemistry of trimethylsilyldiazomethane, it is surprising that thermodynamically favorable N_2 extrusion is not observed. Instead, the only tractable products are the corresponding iron(IV) nitride and iron(II) cyanide complexes, both of which require N=N bond cleavage.

EXPERIMENTAL SECTION

No Uncommon Hazards are Noted. *General Considerations.* All manipulations involving air- or moisture-sensitive compounds and their preparation were performed under an inert atmosphere of dry N_2 by standard Schlenk techniques or in an M. Braun glovebox. The glassware used was oven-dried for at least 12 h at 140 °C before use. Celite was oven-dried for 12 h at 140 °C. All solvents were purchased from Sigma-Aldrich and used after being dried using alumina and Q5 drying columns. Trimethylsilyldiazomethane (2 M in hexanes) was purchased from Alfa and was used as received. The compounds PhB(AdIm)$_3$FeCl, PhB(AdIm)$_3$FeN$_2$,[19] Gomberg's dimer,[30] and lithium(trimethylsilyl)diazomethane[31] were prepared according to literature procedures. Deuterated solvents were purchased from Cambridge isotope laboratories. C_6D_6 and THF-d_8 were degassed and stored over molecular sieves for at least 1 day before use. All other compounds purchased from commercial vendors and used as received.

^{1}H NMR spectroscopic measurements of air- and moisture-sensitive compounds were made in J-Young NMR tubes, with the spectroscopic data recorded on Varian 400 MHz NMR and 500 MHz NMR spectrometers at 25 °C. UV−visible spectra were recorded with an Agilent Cary 60 UV−visible spectrometer. IR spectra were recorded with a PerkinElmer IR Spectrometer. Mass spectra were recorded using negative/positive electrospray ionization on a Thermo Electron Corp MAT-95XP spectrometer.

https://doi.org/10.1021/acs.inorgchem.4c00604
Inorg. Chem. XXXX, XXX, XXX−XXX

Samples for ^{57}Fe Mössbauer spectroscopy were prepared by suspending approximately 50 mg of the sample in Paratone N cryoprotectant oil and loaded under liquid N_2. Spectra were obtained using a See Co. (Minneapolis, MN) constant-acceleration spectrometer equipped with a Janis SHI-4 cryostat. Isomer shifts (δ) are reported relative to a 25 μm thick sample of α-Fe foil at 298 K. Data processing and fitting routines were performed using the WMOSS-4F software package.[32]

Magnetic Measurements and Analyses. Magnetic data were collected on a Quantum Design MPMS3 SQUID magnetometer at the Analytical Resources Core at Colorado State University. Measurements were obtained with microcrystalline powder restrained in frozen eicosane within polycarbonate capsules wrapped in Kapton tape and secured in a straw. The prepared straw sample was transported under N_2 in a jar sealed with Teflon (PTFE) tape and electrical tape until quickly transferred into the magnetometer. Magnetic data were collected in the magnetic fields ranging from 0 to 7 T and temperatures from 2 to 300 K. Variable-field magnetization data collected from 0 to 3 T at 100 K revealed a linear field dependence, precluding ferromagnetic impurities for this highly air-sensitive iron-containing compound (Figure S18). Susceptibility data were corrected for complex and eicosane diamagnetism.[33] Susceptibility and magnetization data were analyzed with PHI v3.1.6.[34]

Computational Details. All DFT calculations were performed as implemented in the ORCA 5.0.4 computational software package.[35] The structures of **2**, **3**, and **4** were optimized in the gas phase with the B3LYP functional, def2-SVP[36] basis set, and D3BJ dispersion corrections.[37] Auxiliary basis sets were automatically generated.[38] All structures were verified to be minima on the potential energy surface by frequency calculations. Reevaluation of the electronic energies (single point energy corrections) was done with the triple-ζ basis set def2-TZVP.[2] The ^{57}Fe Mössbauer spectroscopic parameters were calculated using DFT (B3LYP/def2-TZVP) with the CP(PPP) basis set for Fe and calibrated according to the method of Neese.[39]

Synthesis of Complexes. *PhB(AdIm)$_3$FeNH$_2$.* A 20 mL scintillation vial was charged with PhB(AdIm)$_3$FeCl (72 mg, 0.07 mmol) and THF (10 mL). A suspension of sodium amide (14 mg, 0.21 mmol) in THF was added to the solution and the mixture stirred overnight. The solvent was removed from the off-white reaction mixture in vacuo, and the resulting residue extracted into toluene and filtered through Celite. The toluene was removed under vacuum to afford an off-white solid that was used without further purification (92% yield). ^{1}H NMR (C_6D_6, 400 MHz): δ 76 (3H, Im-H), 69 (3H, Im-H), 51 (2H, B(C_6H_5) *o*/*m*-H), 25 (2H, B(C_6H_5) *o*/*m*-H), 21 (1H, B(C_6H_5) *p*-H), −55 (Ad, 18H).; MS: m/*Z* [M+2H]$^+$ Calculated for $C_{45}H_{58}N_7BFe$ 765.4215; found 765.4111. μ_{eff} = 4.9(0) μ_B.

$$PhB(AdIm)_3Fe(N = N = CSiMe_3) \quad (2)$$

Method 1: In a 20 mL scintillation vial, PhB(AdIm)$_3$FeCl (22 mg, 0.02 mmol) was dissolved in THF (5 mL). A solution of lithium(trimethylsilyl)diazomethane (3 mg, 0.02 mmol) in THF was slowly added dropwise at room temperature. The colorless solution quickly becomes golden in color. After 1 h, the volatiles were removed under vacuum, yielding a golden solid. Crystals suitable for single crystal X-ray diffraction were grown by room temperature vapor diffusion of THF into toluene.

Method 2: In a 20 mL scintillation vial, PhB(AdIm)$_3$FeNH$_2$ (45 mg, 0.05 mmol) was dissolved in THF (10 mL). Trimethylsiyldiazomethane (29 μL, 0.05 mmol, 2 M solution in hexanes) is added via a syringe with stirring. The colorless solution gradually turns golden yellow. After 20 min, the reaction was briefly exposed to vacuum to remove the ammonia byproduct. The reaction was stirred for 1 h and periodically exposed to vacuum. The solvent was slowly removed under vacuum to yield a golden-yellow solid. Crystals suitable for single crystal X-ray diffraction were grown by room temperature vapor diffusion of THF into toluene.

Method 3: A J-Young tube was charged with PhB(AdIm)$_3$Fe(*N*,*N*′-k^2-N_2CSi(CH$_3$)$_3$) (10 mg, 0.01 mmol) and C_6D_6 (0.5 mL). A solution of Gomberg's dimer (5 mg, 0.01 mmol) in minimal C_6D_6 was added to the tube. Over the course of 10 min, the red solution gradually becomes golden-yellow, with the product characterized by ^{1}H NMR spectroscopy. This transformation can also be accomplished by stoichiometric reaction with TEMPO.

^{1}H NMR (C_6D_6, 400 MHz) δ 74 (3H, Im-H), 69 (3H, Im-H), 47 (2H, B(C_6H_5) *o*/*m*-H), 34 (9H, Si(CH$_3$)$_3$), 23 (2H, B(C_6H_5) *o*/*m*-H), 20 (1H, B(C_6H_5) *p*-H), 3 (Ad, 18H), −38 (Ad, 18H). ESI-MS: *m*/*z* [M]$^+$ Calculated for $C_{49}H_{65}N_8BFeSi$ 860.4538; found 860.4521. μ_{eff} = 5.0(2) μ_B IR (KBr): $\nu_{N=N}$ = 2047 cm^{-1}.

Due to the light sensitivity of this complex, its ^{1}H NMR spectra often show resonances from **6** and **7** impurities. In addition, resonances from **3** are usually observed due to the reaction of **2** with additional LiTMSD.

$$PhB(AdIm)3Fe(C = N = NSiMe_3) \quad (3)$$

Method 1: In a 20 mL scintillation vial, PhB(AdIm)$_3$FeCl (68 mg, 0.05 mmol) is dissolved in THF with stirring. Lithium(trimethylsilyl)-diazomethane (21 mg, 0.11 mmol) in minimal THF was slowly added dropwise to form a golden yellow solution. The reaction darkened slightly after 24 h stirring. The volatiles were removed under vacuum to afford a yellow solid. Fine yellow crystals suitable for single crystal X-ray diffraction were afforded by reverse vapor diffusion of THF solution of the product into a bath of toluene (66% yield).

Method 2: A J-Young tube was charged with **2** (9 mg, 0.01 mmol) and THF-d_8 (0.5 mL) followed by a solution of lithium-(trimethylsilyl)diazomethane (∼1 mg, 0.01 mmol) in minimal THF-d_8. The reaction was monitored by ^{1}H NMR spectroscopy, with isomerization to PhB(AdIm)$_3$Fe(C$\underline{N}_2$−SiMe$_3$) occurring overnight.

^{1}H NMR (C_6D_6, 400 MHz) δ 71 (3H, Im-H), 52 (3H, Im-H), 32 (2H, B(C_6H_5) *o*/*m*-H), 17 (2H, B(C_6H_5) *o*/*m*-H), 16 (9H, Si(CH$_3$)$_3$), 15 (1H, B(C_6H_5) *p*-H), 3 (Ad, 18H), −19 (Ad, 18H). ESI-MS: *m*/*z* [MH]$^+$ Calculated for $C_{49}H_{66}N_8BFeSi$ 861.4617; found 861.4629. μ_{eff} = 4.9(9) μ_B. IR (KBr): $\nu_{N=N}$ = 2062 cm^{-1}.

PhB(AdIm)$_3$Fe(N,N′-k^2-N=N=CHSi(CH$_3$)$_3$) (**5**). In a 20 mL scintillation vial, PhB(AdIm)$_3$FeN$_2$ (54 mg, 0.06 mmol) was dissolved in THF (10 mL). Trimethylsilyldiazomethane (35 μL, 0.06 mmol; 2 M in hexanes) was added via a syringe with stirring. The solution darkened from green to dark red with effervescence. Following 1 h stirring, the solution was dried under vacuum to afford a brown solid, which was washed with pentane. Small brown crystals suitable for single crystal X-ray diffraction were grown by slow evaporation of benzene at room temperature ^{1}H NMR (C_6D_6, 400 MHz) δ 50 (3H, Im-H), 39 (3H, Im-H), 26 (2H, B(C_6H_5) *o*/*m*-H), 14 (2H, B(C_6H_5) *o*/*m*-H), 13 (2H, B(C_6H_5) *p*-H), 9 (9H, Si(CH$_3$)$_3$), 3 (Ad, 18H), −13 (Ad, 18H). IR (KBr): $\nu_{N=N}$ = 2059 cm^{-1}. The air sensitivity of this product has hindered efforts to obtain high resolution mass spectrometry data.

PhB(AdIm)$_3$FeF. A 20 mL scintillation vial was charged with PhB(AdIm)$_3$FeCl (57 mg, 0.07 mmol) and THF (10 mL). A slurry of tetramethylammonium fluoride (14 mg, 0.21 mmol) in THF (∼10 mL) was added, and the mixture was stirred overnight. The solvent was removed from resulting pale-yellow slurry in vacuo, and the residue was extracted with toluene and filtered through Celite. The toluene was removed under vacuum to afford a pale yellow solid. Crystals suitable for X-ray diffraction were produced by the reverse vapor diffusion of a concentrated THF solution of the resulting material into a bath of toluene. ^{1}H NMR (C_6D_6, 400 MHz) δ 74 (3H, Im-H), 71 (3H, Im-H), 49 (2H, B(C_6H_5) *o*/*m*-H), 24 (2H, B(C_6H_5) *o*/*m*-H), 20 (2H, B(C_6H_5) *p*-H), −44 (Ad, 18H). μ_{eff} = 4.9(9) μ_B ESI-MS: *m*/*z* [M]$^+$ Calculated for $C_{45}H_{57}N_6BFFe$ 767.4066; found 767.4041.

PhB(AdIm)$_3$Fe−C≡N (**6**). A 20 mL scintillation vial was charged with PhB(AdIm)$_3$FeF (20 mg, 0.07 mmol) and THF (10 mL). A solution of trimethylsilyl cyanide (5 μL, 0.21 mmol) in THF (2 mL) was added, and the reaction was stirred for 10 min. The volatiles were removed from the salmon-colored solution in vacuo. ^{1}H NMR (C_6D_6, 400 MHz) δ 77 (3H, Im-H), 72 (3H, Im-H), 49 (2H, B(C_6H_5) *o*/*m*-H), 16 (2H, B(C_6H_5) *o*/*m*-H), 14 (1H, B(C_6H_5) *p*-H), −14 (Ad, 18H). MS: *m*/*z* [M]$^+$ Calculated for $C_{45}H_{58}N_6BFe$ 761.4034; found

https://doi.org/10.1021/acs.inorgchem.4c00604
Inorg. Chem. XXXX, XXX, XXX−XXX

761.4051. μ_{eff} = 4.8(9) μ_B IR (KBr): ν_{CN} = 2051 cm^{-1}. The trimethylsilylfluoride byproduct was observed in a separate NMR scale experiment. ^{19}F NMR (C_6D_6) δ −158 (s).

PhB(AdIm)$_3$FeN$_3$. A 20 mL scintillation vial was charged with PhB(AdIm)$_3$FeCl (57 mg, 0.07 mmol) and THF (10 mL). A suspension of sodium azide (14 mg, 0.21 mmol) in THF (10 mL) was then added. The mixture was stirred for 2 d to yield an off-white reaction mixture. The solvent was evaporated in vacuo, and the resulting residue was extracted into toluene and filtered through Celite. The toluene was removed under vacuum to afford an off-white solid. ^1H NMR (C_6D_6, 400 MHz) δ 73 (3H, Im-H), 63 (3H, Im-H), 43 (2H, B(C_6H_5) *o*/*m*-H), 21 (2H, B(C_6H_5) *o*/*m*-H), 18 (2H, B(C_6H_5) *p*-H), −32 (Ad, 18H). IR (KBr): $\nu_{N=N=N}$ = 2068 cm^{-1}. The compound was used without further purification.

*PhB(AdIm)$_3$Fe≡N (**7**).* A 250 mL quartz round-bottom flask was charged with PhB(AdIm)$_3$FeN$_3$ (40 mg) and THF (20 mL) with stirring. The flask was sealed with a vacuum adaptor, removed from the glovebox, and photolyzed with stirring for 1.5 h. During this time, the solution changed from colorless to bright red. The volatiles were removed under vacuum to afford a red solid. Crystals suitable for X-ray diffraction were produced by reverse vapor diffusion of THF from a solution of the red material into a toluene bath at room temperature. ^1H NMR (C_6D_6, 400 MHz) δ 7.96 (d, 2H, B(C_6H_5) *o*-H), 7.29 (m, 3H, B(C_6H_5) *p*/*m*-H), 7.00 (s, 3H, Im-H), 6.71 (s,3H, Im-H), 2.66 (s, 18H Ad), 2.03 (d, 9H, Ad), 1.68 (d, 9H, Ad), 1.50 (d, 9H, Ad). UV−vis (THF, 25 °C) λ_{max} = 480 nm MS: m/Z $[M]^+$ Calculated for $C_{45}H_{56}N_7BFe$ 761.4034; found 761.4051.

Photochemical Transformations. *Photolysis of **2**.* A J-Young tube was charged with **2** (12 mg) and C_6D_6 (0.5 mL). The solution was photolyzed with a XeHg broadband lamp (800 W) for 30 min at 25 °C, during which time the golden yellow solution turned a brilliant salmon color. ^1H NMR spectra were collected periodically during this time, revealing the formation of **6** and **7** (Figure S8).

*Photolysis of **3**.* A J-Young tube was charged with **3** (14 mg) and C_6D_6 (0.5 mL). The solution was photolyzed with a XeHg broadband lamp (800 W) at 25 °C. Full consumption of the starting complex occurred within 5 min with the golden-yellow solution evolving to a pale-off-white color. ^1H NMR spectroscopy reveals the formation of **6** and an unidentified paramagnetic species having 3-fold symmetry.

*Photolysis of **5**.* A J-Young tube was charged with **5** (10 mg) and C_6D_6 (0.5 mL) and photolyzed with a XeHg broadband lamp (800 W for 90 min at 25 °C). ^1H NMR spectra were collected periodically during this time, revealing the formation of **6** and **7** (Figure S9).

The reaction was also conducted on synthetic scale. A 50 mL side arm Schlenk flask was charged with a stir-bar, **5** (50 mg, 0.05 mmol) and THF (15 mL). The reaction was photolyzed with a XeHg broadband lamp (800 W for 130 min at 25 °C). The solution was dried under vacuum, and the resulting red solid was washed with pentane until the washings ran clear. The solid was then dissolved in minimal THF and crystallized by reverse vapor diffusion into a toluene bath at room temperature yielding crystals of disordered **6** and **7**.

■ ASSOCIATED CONTENT

Supporting Information

The Supporting Information is available free of charge at https://pubs.acs.org/doi/10.1021/acs.inorgchem.4c00604.

Additional experimental and computational details; tables with crystallographic parameters; and ^1H NMR and mass spectrometry spectra of complexes (PDF)

DFT-optimized coordinates (XYZ)

Accession Codes

CCDC 2331643 and 2331954−2331958 contain the supplementary crystallographic data for this paper. These data can be obtained free of charge via www.ccdc.cam.ac.uk/data_request/cif, or by emailing data_request@ccdc.cam.ac.uk, or by contacting The Cambridge Crystallographic Data Centre, 12 Union Road, Cambridge CB2 1EZ, UK; fax: +44 1223 336033.

■ AUTHOR INFORMATION

Corresponding Author

Jeremy M. Smith − *Department of Chemistry, 800 E. Kirkwood Ave, Indiana University, Bloomington, Indiana 47405, United States;* orcid.org/0000-0002-3206-4725; Email: smith962@indiana.edu

Authors

Austin D. Chivington − *Department of Chemistry, 800 E. Kirkwood Ave, Indiana University, Bloomington, Indiana 47405, United States*

Sammie Squire − *Department of Chemistry, 800 E. Kirkwood Ave, Indiana University, Bloomington, Indiana 47405, United States*

Nobuyuki Yamamoto − *Department of Chemistry, 800 E. Kirkwood Ave, Indiana University, Bloomington, Indiana 47405, United States*

Maren Pink − *Department of Chemistry, 800 E. Kirkwood Ave, Indiana University, Bloomington, Indiana 47405, United States;* orcid.org/0000-0001-9049-4574

Morgan D. Griffith − *Department of Chemistry, Colorado State University, Fort Collins, Colorado 80523, United States; Department of Chemistry and Biochemistry, The Ohio State University, Columbus, Ohio 43210, United States*

Jess Fletcher − *Department of Chemistry and Biochemistry, The Ohio State University, Columbus, Ohio 43210, United States*

Yafei Gao − *Department of Chemistry, 800 E. Kirkwood Ave, Indiana University, Bloomington, Indiana 47405, United States;* orcid.org/0000-0001-7970-8535

Joseph M. Zadrozny − *Department of Chemistry, Colorado State University, Fort Collins, Colorado 80523, United States; Department of Chemistry and Biochemistry, The Ohio State University, Columbus, Ohio 43210, United States;* orcid.org/0000-0002-1309-6545

Complete contact information is available at: https://pubs.acs.org/10.1021/acs.inorgchem.4c00604

Notes

The authors declare no competing financial interest.

■ ACKNOWLEDGMENTS

Funding from the NSF is gratefully acknowledged by A.D.C., S.S., and J.M.S. (CHE-1900020). J.M.Z. and M.D.G. acknowledge the NIH (1R35GM150894) for support.

■ REFERENCES

(1) (a) Mindiola, D. J.; Hillhouse, G. L. Synthesis, Structure, and Reactions of a Three-Coordinate Nickel-Carbene Complex, {1,2-Bis(di-*tert*-butylphosphino)ethane}Ni = CPh_2. *J. Am. Chem. Soc.* **2002**, *124*, 9976−9977. (b) Iluc, V. M.; Hillhouse, G. L. Three-Coordinate Nickel Carbene Complexes and Their One-Electron Oxidation Products. *J. Am. Chem. Soc.* **2014**, *136*, 6479−6488.

(2) Dartiguenave, M.; Menu, M. J.; Deydier, E.; Dartiguenave, Y.; Siebald, H. Crystal and Molecular Structures of Transition Metal Complexes with N- and C-bonded Diazoalkane Ligands. *Coord. Chem. Rev.* **1998**, *178*−*180*, 623−663.

(3) Regitz, M.; Maas, G. Structure and Spectroscopic Properties. In *Diazo Compounds*; Academic Press, 1986; pp 3−64.

(4) (a) Cowley, R. E.; Bontchev, R. P.; Sorrell, J.; Sarracino, O.; Feng, Y.; Wang, H.; Smith, J. M. Formation of a Cobalt(III) Imido

from a Cobalt(II) Amido Complex. Evidence for Proton-Coupled Electron Transfer. *J. Am. Chem. Soc.* **2007**, *129*, 2424−2425. (b) Ding, M.; Cutsail, G. E., III; Aravena, D.; Amoza, M.; Rouzières, M.; Dechambenoit, P.; Losovyj, Y.; Pink, M.; Ruiz, E.; Clérac, R.; Smith, J. M. A Low Spin Manganese(IV) Nitride Single Molecule Magnet. *Chem. Sci.* **2016**, *7*, 6132−6140. (c) Goetz, M. K.; Hill, E. A.; Filatov, A. S.; Anderson, J. S. Isolation of a Terminal Co(III)-Oxo Complex. *J. Am. Chem. Soc.* **2018**, *140*, 13176−13180. (d) Goetz, M. K.; Schneider, J. E.; Filatov, A. S.; Jesse, K. A.; Anderson, J. S. Enzyme-Like Hydroxylation of Aliphatic C−H Bonds From an Isolable Co-Oxo Complex. *J. Am. Chem. Soc.* **2021**, *143*, 20849−20862.

(5) Valdez-Moreira, J. A.; Beagan, D. M.; Yang, H.; Telser, J.; Hoffman, B. M.; Pink, M.; Carta, V.; Smith, J. M. Hydrocarbon Oxidation by an Exposed, Multiply Bonded Iron(III) Oxo Complex. *ACS Cent. Sci.* **2021**, *7*, 1751−1755.

(6) Nieto, I.; Ding, F.; Bontchev, R. P.; Wang, H.; Smith, J. M. Thermodynamics of Hydrogen Atom Transfer to a High Valent Iron Imido Complex. *J. Am. Chem. Soc.* **2008**, *130*, 2716−2717.

(7) Valdez-Moreira, J. A.; Wannipurage, D. C.; Pink, M.; Carta, V.; Moënne-Loccoz, P.; Telser, J.; Smith, J. M. Hydrogen Atom Abstraction by a High-Spin [Fe^{III}=S] Complex. *Chem* **2023**, *9*, 2601−2609.

(8) (a) Scepaniak, J. J.; Fulton, M. D.; Bontchev, R. P.; Duesler, E. N.; Kirk, M. L.; Smith, J. M. Structural and Spectroscopic Characterization of an Electrophilic Iron Nitrido Complex. *J. Am. Chem. Soc.* **2008**, *130*, 10515−10517. (b) Scepaniak, J. J.; Young, J. A.; Bontchev, R. P.; Smith, J. M. Formation of Ammonia from an Iron Nitrido Complex. *Angew. Chem., Int. Ed.* **2009**, *48*, 3158−3160. (c) Scepaniak, J. J.; Vogel, C. S.; Khusniyarov, M. M.; Heinemann, F. W.; Meyer, K.; Smith, J. M. Synthesis, Structure, and Reactivity of an Iron(V) Nitride. *Science* **2011**, *331*, 1049−1052. (d) Smith, J. M.; Subedi, D. The Structure and Reactivity of Iron Nitride Complexes. *Dalton Trans.* **2012**, *41*, 1423−1429. (e) Martinez, J. L.; Lin, H.-J.; Lee, W.-T.; Pink, M.; Chen, C.-H.; Gao, X.; Dickie, D. A.; Smith, J. M. Cyanide Ligand Assembly by Carbon Atom Transfer to an Iron Nitride. *J. Am. Chem. Soc.* **2017**, *139*, 14037−14040.

(9) Reesbeck, M. E.; Grubel, K.; Kim, D.; Brennessel, W. W.; Mercado, B. Q.; Holland, P. L. Diazoalkanes in Low-Coordinate Iron Chemistry: Bimetallic Diazoalkyl and Alkylidene Complexes of Iron(II). *Inorg. Chem.* **2017**, *56*, 1019−1022.

(10) Bart, S. C.; Bowman, A. C.; Lobkovsky, E.; Chirik, P. J. Iron Diazoalkane Chemistry: N-N Bond Hydrogenation and Intramolecular C-H Activation. *J. Am. Chem. Soc.* **2007**, *129*, 7212−7213.

(11) Aghazada, S.; Miehlich, M.; Messelberger, J.; Heinemann, F. W.; Munz, D.; Meyer, K. A Terminal Iron Nitrilimine Complex: Accessing the Terminal Nitride through Diazo N−N Bond Cleavage. *Angew. Chem., Int. Ed.* **2019**, *58*, 18547−18551.

(12) (a) Boche, G.; Harms, K.; Marsch, M.; Schubert, F. {6 Lithio(trimethylsilyl)diazomethane· 2 Lithio[4,5-bis(trimethylsilyl)-triazene]· 7 Diethyl Ether}: The First X-Ray Structure Analysis of a Lithiated Diazoalkane. *Chem. Ber.* **1994**, *127*, 2193−2195. (b) Armstrong, D. R.; Davies, R. P.; Haigh, R.; Hendy, M. A.; Raithby, P. R.; Snaith, R.; Wheatley, A. E. H. A Solid-State, Solution, and Theoretical Structural Study of Kinetic and Thermodynamic Lithiated Derivatives of a Simple Diazomethane and Their Reactivities Towards Aryl Isothiocyanates. *Eur. J. Inorg. Chem.* **2003**, *2003*, 3363−3375.

(13) The carbon and nitrogen atom assignments for the trimethylsilylazomethane-derived ligand in structures **2** and **3** were based on the electron densities found in the diffraction measurements. The crystal structures resulted in an agreement between the structural model and the data, evidenced by the lowest possible refinement values achieved.

(14) Mawhinney, R. C.; Muchall, H. M.; Peslherbe, G. H. The electronic structure of nitrilimines revisited. *Chem. Commun.* **2004**, 1862−1863.

(15) Aghazada, S.; Fehn, D.; Heinemann, F. W.; Munz, D.; Meyer, K. Cobalt Diazo-Compounds: From Nitrilimide to Isocyanoamide via a Diazomethanediide Fleeting Intermediate. *Angew. Chem., Int. Ed.* **2021**, *60*, 11138−11142.

(16) (a) Polse, J. L.; Andersen, R. A.; Bergman, R. G. Synthesis, Structure, and Reactivity Studies of an η^2-N_2-Titanium Diazoalkane Complex. Generation and Trapping of a Carbene Complex Intermediate. *J. Am. Chem. Soc.* **1996**, *118*, 8737−8738. (b) Polse, J. L.; Kaplan, A. W.; Andersen, R. A.; Bergman, R. G. Synthesis of an η^2-N_2-Titanium Diazoalkane Complex with Both Imido- and Metal Carbene-Like Reactivity Patterns. *J. Am. Chem. Soc.* **1998**, *120*, 6316−6328.

(17) Rheingold, R. L.; Theopold, K. H. *CCDC 1963923: Experimental Crystal Structure Determination*, 2019.

(18) Russell, S. K.; Hoyt, J. M.; Bart, S. C.; Milsmann, C.; Stieber, S. C. E.; Semproni, S. P.; DeBeer, S.; Chirik, P. J. Synthesis, Electronic Structure and Reactivity of Bis(imino)pyridine Iron Carbene Complexes: Evidence for a Carbene Radical. *Chem. Sci.* **2014**, *5*, 1168−1174.

(19) Fan, Y.; Cheng, J.; Gao, Y.; Shi, M.; Deng, L. Iron Dinitrogen Complexes Supported by Tris(NHC)borate Ligand: Synthesis, Characterization, and Reactivity Study. *Huaxue Xuebao* **2018**, *76*, 445−452.

(20) Chilton, N. F.; Anderson, R. P.; Turner, L. D.; Soncini, A.; Murray, K. S. PHI: A powerful new program for the analysis of anisotropic monomeric and exchange-coupled polynuclear *d*- and *f*-block complexes. *J. Comput. Chem.* **2013**, *34*, 1164−1175.

(21) (a) Hooper, R. X.; Mercado, B. Q.; Holland, P. L. Desulfurization and N_2 Binding at an Iron Complex Derived from the C−S Activation of Benzothiophene. *Organometallics* **2023**, *42*, 2019−2027. (b) MacLeod, K. C.; Vinyard, D. J.; Holland, P. L. A Multi-Iron System Capable of Rapid N_2 Formation and N_2 Cleavage. *J. Am. Chem. Soc.* **2014**, *136*, 10226−10229. (c) Pecak, J.; Stöger, B.; Mastalir, M.; Veiros, L. F.; Ferreira, L. P.; Pignitter, M.; Linert, W.; Kirchner, K. Five-Coordinate Low-Spin {FeNO}^{7} PNP Pincer Complexes. *Inorg. Chem.* **2019**, *58*, 4641−4646.

(22) Horitani, M.; Grubel, K.; McWilliams, S. F.; Stubbert, B. D.; Mercado, B. Q.; Yu, Y.; Gurubasavaraj, P. M.; Lees, N. S.; Holland, P. L.; Hoffman, B. M. ENDOR Characterization of an Iron−Alkene Complex Provides Insight into a Corresponding Organometallic Intermediate of Nitrogenase. *Chem. Sci.* **2017**, *8*, 5941−5948.

(23) Hendrich, M. P.; Gunderson, W.; Behan, R. K.; Green, M. T.; Mehn, M. P.; Betley, T. A.; Lu, C. C.; Peters, J. C. On the Feasibility of N_2 Fixation via a Single-Site Fe^I/Fe^{IV} Cycle: Spectroscopic Studies of $Fe^I(N_2)Fe^I$, $Fe^{IV}N$, and Related Species. *Proc. Natl. Acad. Sci. U.S.A.* **2006**, *103*, 17107−17112.

(24) Speelman, A. L.; Čorić, I.; Van Stappen, C.; DeBeer, S.; Mercado, B. Q.; Holland, P. L. Nitrogenase-Relevant Reactivity of a Synthetic Iron−Sulfur−Carbon Site. *J. Am. Chem. Soc.* **2019**, *141*, 13148−13157.

(25) Agarwal, R.; Coste, S. C.; Groff, B. D.; Heuer, A. M.; Noh, H.; Parada, G. A.; Wise, C. F.; Nichols, E. M.; Warren, J. J.; Mayer, J. M. Free Energies of Proton-Coupled Electron Transfer Reagents and Their Applications. *Chem. Rev.* **2022**, *122*, 1−49.

(26) Tsang, W. Thermodynamic and kinetic properties of the cyclohexadienyl radical. *J. Phys. Chem.* **1986**, *90*, 1152−1155.

(27) Tilset, M.; Parker, V. D. Solution homolytic bond dissociation energies of organotransition-metal hydrides. *J. Am. Chem. Soc.* **1989**, *111*, 6711−6717.

(28) Choi, J.; Pulling, M. E.; Smith, D. M.; Norton, J. R. Unusually Weak Metal-Hydrogen Bonds in $HV(CO)_4$(P-P) and Their Effectiveness as H● Donors. *J. Am. Chem. Soc.* **2008**, *130*, 4250−4252.

(29) Valdez-Moreira, J. A.; Thorarinsdottir, A. E.; DeGayner, J. A.; Lutz, S. A.; Chen, C.-H.; Losovyj, Y.; Pink, M.; Harris, T. D.; Smith, J. M. Strong π-Backbonding Enables Record Magnetic Exchange Coupling Through Cyanide. *J. Am. Chem. Soc.* **2019**, *141*, 17092−17097.

(30) Rosenthal, A. J.; Devillard, M.; Miqueu, K.; Bouhadir, G.; Bourissou, D. A Phosphine-Coordinated Boron-Centered Gomberg-Type Radical. *Angew. Chem., Int. Ed.* **2015**, *54*, 9198−9202.

(31) Evans, W. J.; Montalvo, E.; Champagne, T. M.; Ziller, J. W.; DiPasquale, A. G.; Rheingold, A. L. Organolanthanide-Based

https://doi.org/10.1021/acs.inorgchem.4c00604
Inorg. Chem. XXXX, XXX, XXX−XXX

Synthesis of 1,2,3-Triazoles from Nitriles and Diazo Compounds. *J. Am. Chem. Soc.* **2008**, *130*, 16−17.
(32) Ion Prisecaru, "*WMOSS4Mössbauer Spectral Analysis Software*, www.wmoss.org, 2009−2016.
(33) Bain, G. A.; Berry, J. F. Diamagnetic Corrections and Pascal's Constants. *J. Chem. Educ.* **2008**, *85*, 532−536.
(34) Chilton, N. F.; Anderson, R. P.; Turner, L. D.; Soncini, A.; Murray, K. S. PHI: A Powerful New Program for the Analysis of Anisotropic Monomeric and Exchange-Coupled Polynuclear d- and f-block Complexes. *J. Comput. Chem.* **2013**, *34*, 1164−1175.
(35) Neese, F. Software update: The ORCA program system-Version 5.0. *WIREs Comp. Mol. Sci.* **2022**, *12*, No. e1606.
(36) Weigend, F.; Ahlrichs, R. Balanced Basis Sets of Split Valence, Triple Zeta Valence and Quadruple Zeta Valence Quality for H to Rn: Design and Assessment of Accuracy. *Phys. Chem. Chem. Phys.* **2005**, *7*, 3297−3305.
(37) (a) Grimme, S.; Ehrlich, S.; Goerigk, L. Effect of the Damping Function in Dispersion Corrected Density Functional Theory. *J. Comput. Chem.* **2011**, *32*, 1456−1465. (b) Grimme, S.; Antony, J.; Ehrlich, S.; Krieg, H. J. A Consistent and Accurate *ab initio* Parametrization of Density Functional Dispersion Correction (DFT-D) for the 94 Elements H-Pu. *Chem. Phys.* **2010**, *132*, 154104.
(38) Stoychev, G. L.; Auer, A. A.; Neese, F. Automatic Generation of Auxiliary Basis Sets. *J. Chem. Theory Comput.* **2017**, *13*, 554−562.
(39) Bjornsson, R.; Neese, F.; DeBeer, S. Revisiting the Mössbauer Isomer Shifts of the FeMoco Cluster of Nitrogenase and the Cofactor Charge. *Inorg. Chem.* **2017**, *56*, 1470−1477.

https://doi.org/10.1021/acs.inorgchem.4c00604
Inorg. Chem. XXXX, XXX, XXX−XXX